

CNT-Reinforced Self-Healable Epoxy Dynamic Networks Based on Disulfide Bond Exchange

Cigdem Caglayan, Geonwoo Kim, and Gun Jin Yun*

Cite This: *ACS Omega* 2022, 7, 43480–43491

Read Online

ACCESS |



Metrics & More

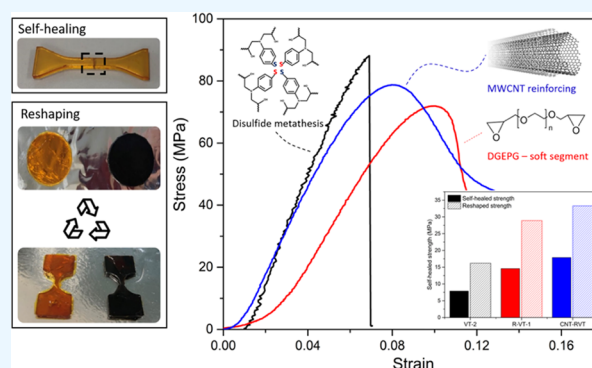


Article Recommendations



Supporting Information

ABSTRACT: The design and utilization of polymers with healing capability have drawn increasing attention owing to their enhanced chain mobility and opportunity to heal minor cracks in composites. Rehealable thermoset polymers promise reduction in the maintenance cost and thus prolonged lifetime, reshaping, and recyclability. Introducing reversible covalent bonds is the mainstay strategy to achieve such plasticity in crosslinked polymers. Herein, we report a dynamic epoxy, which includes associative covalent adaptive networks (CANs) based on disulfide exchange bonds. Epoxy resin is chosen to study rehealing, as it is one of the most critical thermosetting polymers for various industries from aerospace to soft robotics. This study enlightens us about not only the consequences of CANs in the epoxy but also various factors such as soft segments and carbon nanotubes (CNTs). Epoxy dynamic networks are investigated in an attempt to explore the synergistic effect of the soft-segmented resins and CNTs on the healing and reshaping characteristics of epoxy networks along with varying stiffness. This research discusses epoxy dynamic networks in three main aspects: crosslink density, CAN density, and CNTs. Introducing soft segments into the epoxy network enhances the healing efficiency due to the increased chain mobility. A higher CAN density accelerates network rearrangement, improving the healing efficiency. It should also be noted that even with a low weight fraction of nanotubes, CNT-reinforced samples restored their initial strength more than neat samples after healing. The tensile strength of dynamic networks is at least 50 MPa, which is significant for their utility in primary or secondary structural components.



1. INTRODUCTION

The discovery of self-healing materials has driven researchers to investigate reversible bonds in polymeric networks especially in thermoset polymers, which enable new possibilities for various potential applications. Among thermoset polymers, epoxy is a widely used resin due to its high mechanical performance, durability, and creep resistance. Apart from their outstanding mechanical performance, epoxies also exhibit good thermal properties and high chemical resistance. However, there are still challenges to overcome in thermoset epoxy resins, such as their lack of recyclability and reprocessability.^{1–3} Epoxies are subjected to considerable stresses, high temperature, and pressure, which may harm the structural integrity of the composite and reduce the operation lifetime. In the case of an even minimal damage, it is not possible to repair thermosets due to their irreversible covalent bonds. Such a scenario is far from being industry-friendly since the damaged composite part is replaced each time with an excessive maintenance cost.² Using microcapsules inside the polymer has been researched to reduce this cost and unexpected risks. In this concept, the microcapsules get triggered with crack initiation/propagation and release the uncured resin inside the capsule to heal the crack.^{4,5} The drawback of microcapsules is that the process is not reversible and self-healing can be

performed only one time. In addition, it is challenging to maintain microcapsules stabilized during the whole operation time of the composite. Polymers with reversible crosslinks have been proposed broadly in the past two decades, including covalent and noncovalent reversible bonds.^{6–11} The problem with noncovalent interactions is that they are prone to be fragile, which cannot survive under large strains.⁶ Furthermore, there are systems of dissociative reversible covalent adaptive networks (CANs) that depolymerize above a critical temperature and reform new covalent bonds each time.⁶ However, a dissociative CAN system, Diels–Alder as a typical example, is not desirable since it is difficult to maintain the network integrity under such a sudden viscosity drop during the healing process.^{12,13}

Associative covalent adaptive networks overcome the challenges such as reusability and depolymerization owing to

Received: June 22, 2022

Accepted: November 15, 2022

Published: November 24, 2022



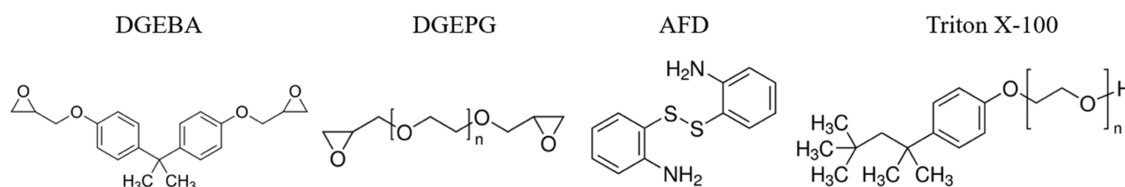


Figure 1. Chemical formula of the materials used to synthesize the epoxy dynamic network.

their constant crosslink density retaining the integrity of the whole structure during the healing process. Among different CAN systems such as transesterification,^{7,9} transcarbamoylation,¹⁴ imine exchange reaction,^{15,16} etc., disulfide metathesis stands out as a leading mechanism within its capability of bond exchange reactions at relatively lower temperatures.^{1,2,7,8,17–20} Li et al.¹⁹ suggested that embedding disulfide dynamic links in epoxy resin, including soft segments, can recover its original strength at least 65% at 80 °C. Despite the achieved high healing efficiency, it should be noted that such a concept demonstrates high flexibility and low mechanical strength, restricting their utility in advanced composites. Canadell et al.²¹ developed an epoxy with disulfide links, which is capable of healing around 80%. The original strength of the sample was limited to 0.6 MPa at most, which cannot be used for any load-bearing structural component. The improvement in the healing of epoxy-based samples was attributed to the adequate mobility for the macroscopic flow using DER732 epoxy resin with low viscosity. Similarly, Lafont et al.²² proved that the increased chain rigidity hampers the healing kinetics, reducing the probability of disulfides to come into contact. On the other hand, Luzuriaga et al.² synthesized a recyclable epoxy resin with a tensile strength of 90 MPa recovering its strength nearly fully after reshaping. In the case of self-healing, this study only monitors a small scratch on the surface of the epoxy instead of a complete failure. Healing of an epoxy sample broken completely in half with a high tensile strength is still open to discussion. To the best of our knowledge, healable epoxy networks studied in the literature either show low strength and elastomer-like behavior^{7,21} or quite the opposite, a very brittle nature.^{23,24} There is a need to understand the comprehensive properties with identical crosslink density and CAN density. Therefore, tailoring the composition of epoxy networks enables a wide range of products, from rubbery to rigid components that are rehealable and recyclable and can be utilized to meet industrial demands.¹⁹

While producing rehealable epoxy networks with adjustable stiffness, it is essential to preserve the mechanical strength in the meantime. Carbon nanotubes (CNTs) come up as a promising solution to increase the mechanical strength^{25–27} and even offer a healing mechanism with multiple stimulation options.^{1,14} Bonab et al.¹⁴ fabricated a CNT-reinforced polyurethane network (TPU) with adaptive covalent bonds and indicated that around 45% of the original strength can be recovered when exposed to microwave radiation. It is noteworthy that the study examines transesterification and carbamate exchange reactions in the TPU system and the tensile strength is limited up to 10 MPa. In addition, there have always been attempts to discover the effects of CNTs on chain mobility and polymerization.^{28,29} For instance, the glass transition temperature is found to be dependent on the existing CNT dispersion media, surfactants, and polymer chemistry.²⁸ Simulations^{20,30} and experiments^{29,31} reveal that CNTs tend to decrease the glass transition temperature and

trigger the activation of the bond exchange reaction at lower temperatures.^{1,14} Such a decrease in the glass transition temperature is ascribed to the reduced crosslinking tendency in the epoxy network in the presence of CNTs.³¹ Similarly, Miyagawa and Drzal³² analyzed the effect of CNTs on the thermophysical properties of the epoxy and observed the same decrease in glass transition temperature linearly by increasing CNT weight ratio. On the other hand, CNTs display a constructive influence on the mechanical strength since CNTs possess a high Young's modulus as a combination of individual moduli of each graphene sheet and the van der Waals forces.^{25,26} To benefit from CNT strength, it is crucial to disperse CNTs in the polymer homogeneously, prepare a stable suspension, and prevent agglomerations, which can act as stress concentration points under an applied load.^{32,33} Applying physical functionalization with a nonionic surfactant is one of the effective methods to improve the interfacial interactions between the CNTs and polymer, enabling the suspension to become more stable.^{34,35}

Consequently, this study elaborates on the effects of more flexible segments and CNTs on epoxy dynamic networks concerning the trade-off between comprehensive properties and healing efficiency. Associative crosslink adaptive networks are embedded into the epoxy resin with disulfide dynamic bonds. Rehealable epoxies are synthesized based on different compositions of resin-to-disulfide molar ratios without any catalyst, as catalysts may cause instability and toxicity.^{2,6,36} For the resin, two different types of commercial resins are used, including hard and soft components. Instead of using only a conventional hard segment resin, it is aimed to tune the stiffness of the epoxy dynamic networks using soft segments.

2. EXPERIMENTAL SECTION

2.1. Materials. Bisphenol A diglycidyl ether (DGEBA, $M_w = 340.41$ g/mol) and poly(ethylene glycol) diglycidyl ether (DGEPG, $M_w = 500$ g/mol) as resins and 2-aminophenyl disulfide (AFD, $M_w = 248.37$ g/mol) and 2,2 ethylenediamine (EDA, $M_w = 212.29$ g/mol) as the hardener are supplied from Sigma-Aldrich. Multiwall carbon nanotubes (CNTs) with a diameter of 110–170 nm and a length of 5–9 μm are supplied from Sigma-Aldrich to synthesize nano-reinforced epoxy dynamic networks. To improve the dispersion and distribution of CNTs in the polymer, Triton X-100 with a critical micelle concentration (CMC) value of 0.22 mM is used as a nonionic surfactant, as shown in Figure 1. Trichlorobenzene (1,2,4) is supplied from Sigma-Aldrich to analyze the chemical resistivity of epoxy networks. All chemicals are analytical grade and used as received without any further process.

2.2. Synthesis of Rehealable and Reformable Epoxy Dynamic Networks. **2.2.1. Synthesis of the Neat Epoxy Dynamic Network.** The crosslinked epoxy dynamic network (VT) is synthesized according to the previous literature.^{1,2} DGEBA and AFD are mixed with different molar ratios at 80 °C for 40 min using a magnetic stirrer and then degassed at 80

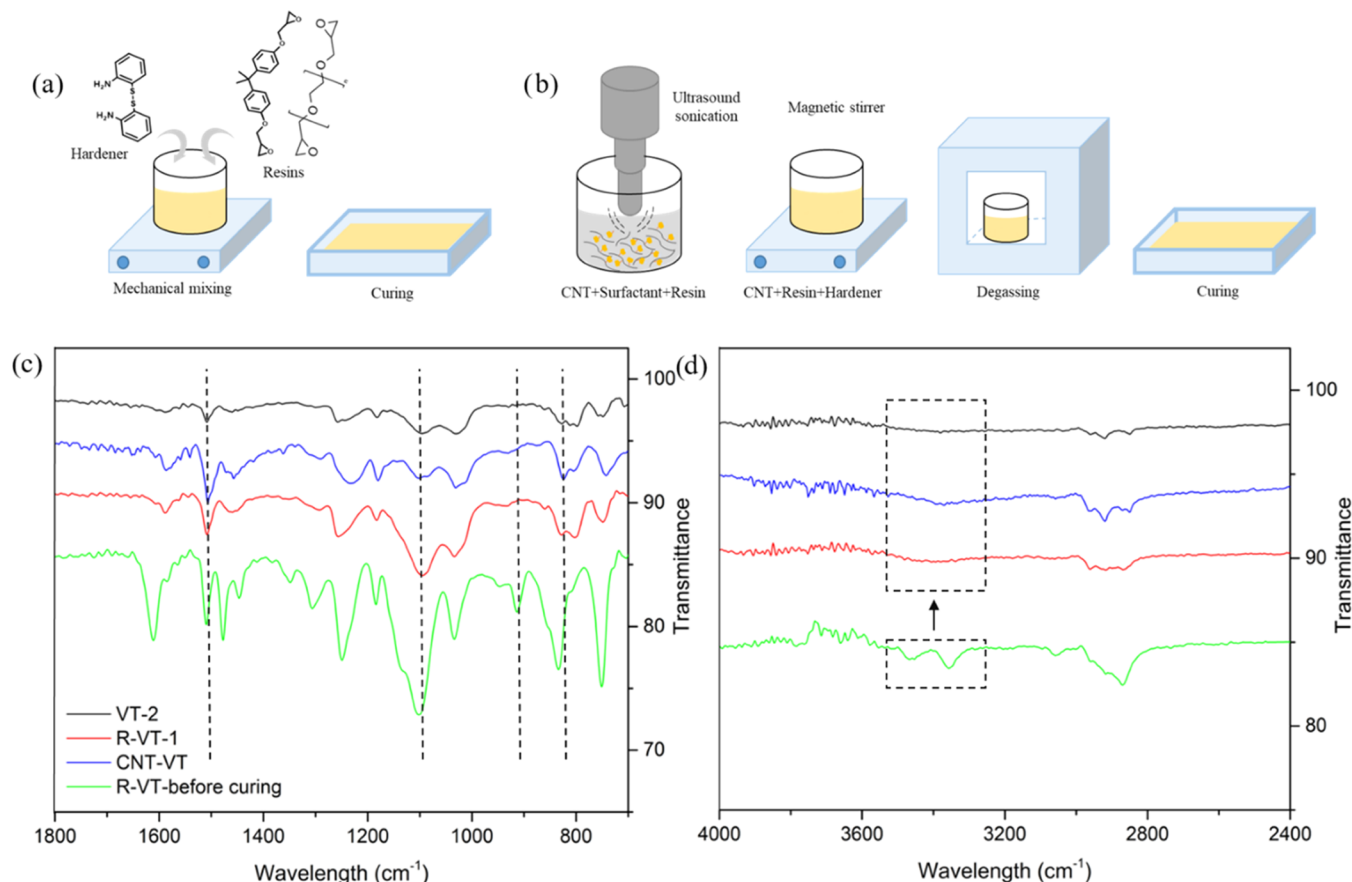


Figure 2. (a) Synthesis of neat and (b) CNT-reinforced epoxy dynamic networks and (c, d) FTIR spectra.

°C for 2 h. The resulting homogeneous liquid is poured into a silicon mold and cured at 150 °C for 10 h in an oven, Figure 2a. Three different compositions are studied as shown in Table 1, where VT-1 represents a stoichiometric ratio, while VT-2 and VT-3 are the ratios promising a better healing performance due to their higher disulfide contents.

Table 1. Compositions of Healable Epoxy Dynamic Networks

sample	DGEBA (mol)	DGEPG (mol)	AFD (mol)	CAN density ^b (wt %)
VT-1	3	0	1.5	26
VT-2	3	0	2	29
VT-3	3	0	2.25	35
R-VT-1	2	1	2	29
R-VT-2	1.8	1.2	2	29
CNT-VT ^a	3	0	2	29
CNT-RVT ^a	2	1	2	29

^aCNT weight fraction is 0.1% for both samples. ^bCAN density stand for disulfide bond density.

2.2.2. Synthesis of the Soft Segment-Introduced Epoxy Dynamic Networks. DGEPG as the soft segment is mixed with DGEBA in different molar ratios at 80 °C. The weighed AFD is then added to the solution, and the whole solution is mixed at 80 °C for 40 min. Herein, to study the effect of soft segments on the healing process, the molar ratio of the epoxy resin to the disulfide hardener is fixed at 3:2. Then, degassing is

performed at 80 °C for 2 h to get rid of bubbles. The resulting epoxy (R-VT) is cured at 150 °C for 10 h in an oven.

2.2.3. Synthesis of the CNT-Reinforced Epoxy Dynamic Networks. In the synthesis of nano-reinforced epoxy dynamic networks, 0.1 wt % CNTs are first dispersed in DGEBA with the help of Triton X-100 (30 CMC, 1 CMC equivalent to a Triton X-100 weight-to-acetone volume ratio of approximately 0.125 mg/mL) by horn sonication, as shown in Figure 2b. Sonication is applied for 30 min at 50% amplitude. The physical adsorption of the surfactant on the CNT surface is expected to lower the surface energy of CNTs and thus prevent the CNT agglomeration inside the polymer. The same procedure is applied also without a surfactant to analyze the differences in the CNT dispersion and distribution. For the CNT-RVT sample, DGEPG is added to the CNT/DGEBA blend, and sonication is performed for 20 min more at 50% amplitude. The weighed AFD is then added to the CNT solution and continued mixing using a magnetic stirrer at 80 °C for 40 min at 300 rpm. The mixture is then degassed at 80 °C for 2 h. CNT-reinforced samples are poured into a silicon mold and cured at 150 °C for 10 h in an oven. All studied compositions can be found in Table 1.

2.2.4. Synthesis of the Reference Epoxy Networks. To confirm the role of disulfide in healing behavior, reference epoxy networks are synthesized replacing AFD with EDA and mixing in a stoichiometric ratio with DGEBA, labeled as Ref-Ep-1. A nonstoichiometric ratio of DGEBA/EDA is also studied to compare the effect of unreacted species on healing, named as Ref-Ep-2. Similarly, another reference epoxy network is synthesized including soft segments, Ref-R-Ep. The

degassing and curing conditions of the reference epoxy networks are the same as those of all other samples. All studied compositions are presented in Table 2.

Table 2. Reference Epoxy Networks without Disulfide Bonds

sample	DGEBA (mol)	DGEPEG (mol)	EDA (mol)
Ref-Ep-1	3	0	1.5
Ref-Ep-2	3	0	2
Ref-R-Ep	2	1	2

2.3. Rehealing and Reshaping Experiments. Samples are first broken completely in half and then joined by applying heat above their glass transition points to achieve mobility, disulfide bond exchange, and hence healing, Figure 8b. The process is carried out in an oven for 1 h to achieve homogeneous heat distribution throughout the samples. Initially, samples with the highest CAN density among VT and R-VT are chosen to be studied under different temperature profiles since they tend to exhibit a higher healing potential. Table S2 presents that a gradual increase in the temperature promotes healing due to easier chain mobility at higher temperatures. Thus, for crosslinked epoxy dynamic networks (VT), the healing temperature is chosen as 180 °C in all presented data, wherein healing is performed at 150 °C for R-VT samples to preserve the structural integrity during the healing process. Reference samples are also treated at 150 and 180 °C for 1 h for Ref-R-Ep and Ref-Ep, respectively. These temperatures are above the glass transition points of all epoxy networks but still relatively low enough to preserve thermal stability. The healing efficiency is defined as the ratio of the healed sample's strength to the original sample's initial strength as given by eq 1.

$$\eta = \frac{\sigma_{\text{healed}}}{\sigma_{\text{original}}} \times 100 \quad (1)$$

Reshaping of epoxy dynamic networks is studied by first preparing small pellets and compressing them in a dog bone-shaped mold under a hot press, Figure 10. R-VT and VT samples are reshaped at 30 MPa pressure for 1 h at 150 and 180 °C, respectively.

3. RESULTS AND DISCUSSION

3.1. Morphological and Thermomechanical Properties of Epoxy Dynamic Networks. The two contradicting aspects crosslink density and CAN density inside the dynamic network should be optimized to enhance the healing performance while retaining the mechanical strength. A relationship between the performed modifications and healing behavior is established by the morphological and thermomechanical characterization of epoxy networks.

3.1.1. Fourier Transform Infrared Spectra. FTIR is conducted with a Thermo-Scientific-Nicolet 6700 to ensure that the samples are fully cured. Figure 2c displays the disappearance of the C–H stretching of epoxide rings at 914 cm^{-1} ,³⁷ showing that the curing process is highly completed. The decreasing intensity in another characteristic vibration peak of the epoxide group at about the 845 cm^{-1} band^{19,37} also proves that curing is complete.

The peaks at 1510 and 1580 cm^{-1} bands remain constant and correspond to the aromatic rings.^{19,38} The band at 1100 cm^{-1} is attributed to the vibration of the C–O–C segment from the aliphatic ether.^{19,39,40} The broad absorption band centered at about 3400 cm^{-1} shown in Figure 2d corresponds to the hydroxyl groups formed by ring opening reactions during the curing process.¹⁹ Also, the peak at 2900 cm^{-1} is related to the aliphatic C–H stretching vibration.³⁹ Full-scale FTIR spectra of Ref-Ep and VT samples can be seen in Figure S1.

3.1.2. Thermogravimetric Analysis. TGA is carried out using a Discovery TA Instruments device in a nitrogen atmosphere to obtain the degradation temperature and hence the overall thermal stability of epoxy networks. A heating rate of 10 °C/min is applied from 25 to 400 °C. Compared to Ref-Ep samples, Figure S4, TGA profiles of dynamic networks have three significant degradation steps characterized by their derivatives, Figure S3b. The first weight loss, around 250 °C, is assigned to the decomposition of oxygen-containing groups. Around 300 °C, disulfide bonds begin to decompose. After 350 °C, a sharp degradation is observed due to epoxy resin pyrolysis.¹⁹

Figure 3a outputs a decrease in the thermal stability of epoxy dynamic networks as the CAN density increases. The presence of disulfide species results in slightly poor degradation behavior since they have a lower bond energy than that of carbon–carbon bonds.²⁴ Less energy is required to decompose the

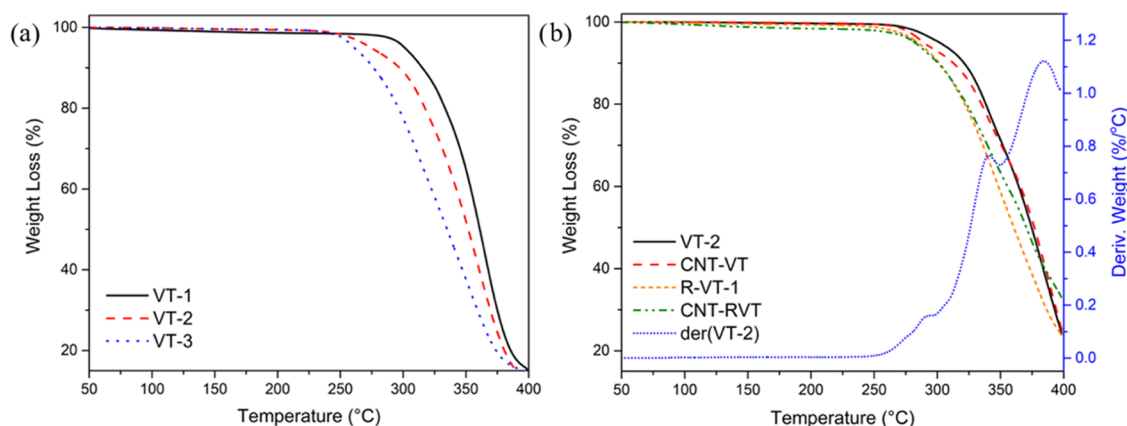
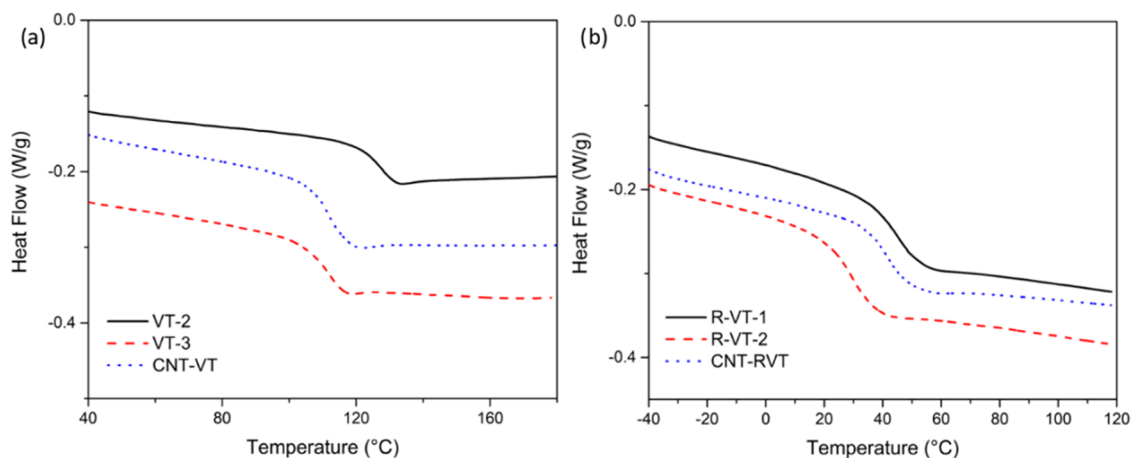


Figure 3. TGA weight loss thermographs of epoxy dynamic networks (a) with respect to increasing CAN density and (b) CNT-reinforced samples and their counterparts.

Table 3. Thermal Properties of Epoxy Networks

sample	VT-2	VT-3	CNT-VT	R-VT-1	R-VT-2	CNT-RVT
T_g (°C)	122.4	109.8	111.3	46.3	35.9	44.4
1% weight loss (°C)	268.88		264.94	240.85		220.3
5% weight loss (°C)	301.72		289.09	284.46		282.21
Δc_p (J/g·K)	0.0069	0.0094	0.0105	0.0110	0.0127	0.0113

**Figure 4.** DSC curves of (a) crosslinked and (b) soft segment-introduced epoxy dynamic networks.

chemical bonds when more S–S bonds are present in the epoxy network. VT-3 exhibits the lowest decomposition temperature owing to its higher CAN density, wherein VT-1 is the most stable network thermally.¹⁹ Since VT-2 and VT-3 samples are synthesized with a nonstoichiometric ratio, the effect of crosslink density is also studied to confirm the major reason for the depression in degradation temperature. Stoichiometric and nonstoichiometric reference epoxy networks, Ref-Ep-1 and Ref-Ep-2, respectively, are subjected to TGA. Considering the result in Figure S4, CAN density is determined to be the driving force of the change in the degradation behavior of VT samples. Likewise, the soft segment-introduced epoxy dynamic network (R-VT-1) illustrates lower thermal stability than that of its counterpart, VT-2, as given in Table 3. The lower thermal stability is related with the soft segments since DGEPA starts decomposing earlier than DGEBA due to its aliphatic polymer chain backbone having less heat resistance.⁴¹ In the case of CNT-reinforced networks, thermal decomposition starts earlier than for their counterparts, Figure 3b. This shows that reinforcing the dynamic networks with CNTs increases the heat diffusion and hence initiates a slightly faster degradation.⁴² The lower decomposition temperature of the CNT-reinforced epoxy can also be linked to the reduced crosslink density, as presented in Table S1. Such a loss in crosslink density is attributed to the decreased crosslinking tendency³¹ due to the penetration of CNTs in free volumes and a large amount of interphase region between the CNTs and polymer.^{30,32}

3.1.3. Differential Scanning Calorimetry. DSC analysis is conducted using a Discovery TA Instruments device. Measurements are recorded at a heating rate of 10 °C/min from –40 to 120 °C for R-VT samples and from 40 to 200 °C for VT samples under a nitrogen atmosphere. DSC curves demonstrated in Figure 4 correspond to a second heating after cooling. The curing state of the epoxy samples is also addressed from the first heating ramp of nonisothermal DSC and from isothermal DSC. According to Figure S5f, no

exothermic peak is observed, confirming that the process time and temperature are enough for the complete curing of epoxy samples. T_g values are determined from the midpoint of the step in the heat flow curves, Table 3. The glass transition temperature for the Ref-Ep-2 sample is detected as 120.5 °C from Figure S5e.

Figure 4a clarifies that the T_g value of the epoxy dynamic network decreases as the disulfide content increases. A higher amount of disulfide exchange bonds imparts easier segmental mobility since they break and reform in numerous sites. According to Table 3 and Figure 4b, it is clear that R-VT samples possess a lower glass transition trend compared to that of VT samples. The significant decrease in T_g values is associated with increasing soft segment molar ratio since it refers to more aliphatic branching chains and higher flexibility.⁴¹

The lower glass transition temperature in CNT-reinforced samples shows the enhanced polymer segmental mobility.^{28,31} The presence of CNTs in the free volume of the polymer reduces the crosslink density,³¹ leading to a decrease in T_g . Another reason for such a decrease in the glass transition temperature of CNT-reinforced epoxy dynamic networks is the high thermal conductivity. It is assumed that introducing CNTs into the epoxy matrix might increase the internal heat diffusion inside the polymer by generating three-dimensional (3D) heat conduction pathways.^{42,43} Such effects of CNTs on the glass transition temperature are well known from previous studies.^{1,30,44}

The mobility of the chains can also be inferred from the heat capacity increase (Δc_p) at glass transition as a measure of the fraction of polymer chains involved in glass transition.^{45–47} The calculation of Δc_p from DSC can be found in the Supporting Information. Among VT samples, Table 3, the heat capacity increase of VT-2 is found to be the lowest, as it forms the strongest crosslinked network, Table S1, having the stoichiometric ratio. VT-3 shows a higher Δc_p , indicating that a higher amount of polymer chains is free of molecular

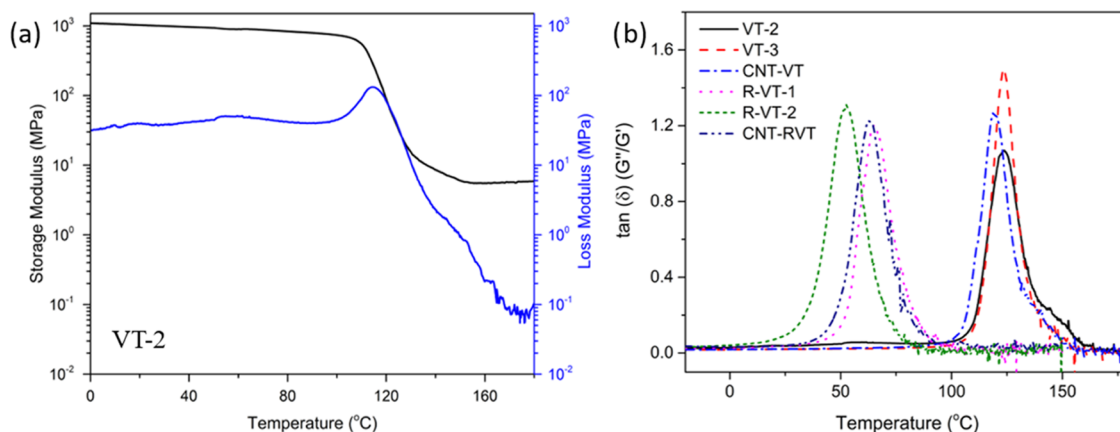


Figure 5. (a) DMA curve of the VT-2 sample representing storage and loss modulus and (b) $\tan \delta$ curves.

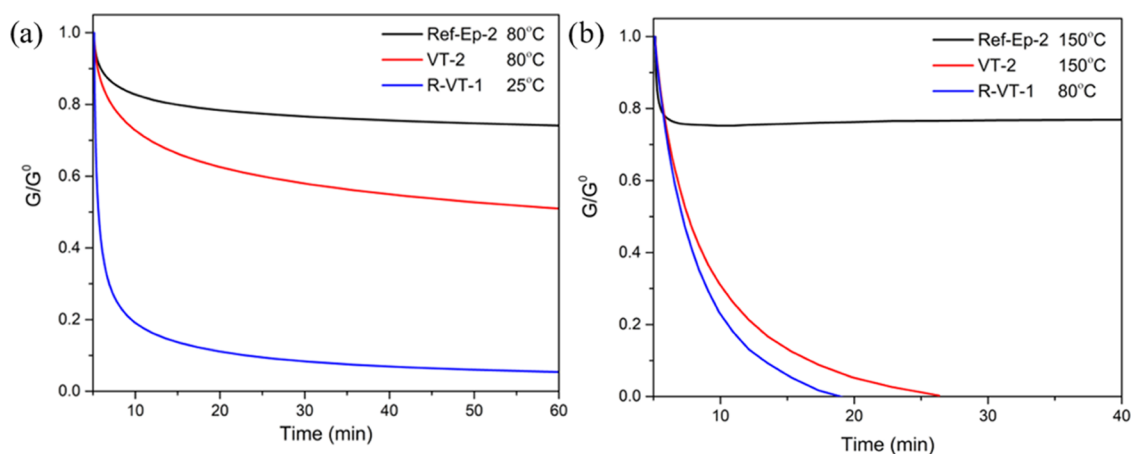


Figure 6. Normalized stress relaxation curves of the epoxy reference and dynamic networks (a) below T_g and (b) above T_g .

motion and participates in glass transition. The higher Δc_p values in R-VT samples are interpreted as the lower restriction of segmental motion as a result of the increased aliphatic chains. CNT samples revealed a higher Δc_p than that of their counterparts, referring to the decreased crosslink density in both cases. Having a higher Δc_p offers a higher healing efficiency since mobility and healing are proportional.

3.1.4. Dynamic Mechanical Analysis. DMA is performed in the tension mode using a Mettler Toledo DMA/SDTA model to address the viscoelastic behavior of epoxy dynamic networks. DMA is applied to $3 \times 5 \times 20 \text{ mm}^3$ (thickness, width, length) samples with a force amplitude of 5 N, a displacement amplitude of $5 \mu\text{m}$, and a frequency of 1 Hz. The loss modulus profile of all epoxies follows a lower trend compared to that of storage modulus, verifying the viscoelastic behavior. Furthermore, all samples follow a stable storage modulus trend in both glassy and rubbery states.

Figure S7 shows that CNT-reinforced samples exhibit a slightly higher storage modulus than that of their neat counterparts. The higher initial storage modulus of the CNT-reinforced epoxy networks refers to the polymer chain motion restriction due to the particle–particle and particle–polymer interactions at room temperature.⁴⁸ Increasing the temperature for CNT-reinforced samples is expected to contribute to the internal heating of the polymer faster and trigger the Brownian motion of CNTs, promoting mobility easier than for neat samples.⁴⁹ R-VT-1 displays a lower storage modulus than that of VT-2, indicating its less-rigid structure.⁵⁰

The flexibility in R-VT samples promises higher healing performance and improved toughness. In Figure 5b, comparing the peak values of $\tan \delta$ (loss factor) curves, VT-3 and CNT-VT samples have a higher loss factor than that of VT-2. R-VT-2 and CNT-RVT also exhibit a slightly higher loss factor than that of the R-VT-1 sample. This indicates higher healing potential since lower viscosity means more segmental motion and bond exchange.

3.1.5. Stress Relaxation. Stress relaxation is conducted using a DMA Q800, TA Instruments. The samples with a size of $3 \times 13 \times 35 \text{ mm}^3$ are measured at a strain of 1% in the linear region, and the relaxation of epoxy networks is monitored as a function of time for 1 h. Time- and temperature-dependent behaviors of epoxy networks are studied carefully to validate the relaxation behavior of dynamic epoxy networks with reversible covalent networks. The studied temperature profiles are chosen to compare the relaxation behavior of dynamic networks below and above their glass transition points.

Figure 6 shows that epoxy dynamic networks are able to flow in all cases and attain a less stretched form due to the disulfide exchange mechanism. Comparing Ref-Ep and VT-2 samples, there is no obvious relaxation behavior in the Ref-Ep-2 sample, signifying the importance of disulfide exchange bonds in the epoxy network. Both VT-2 and R-VT-1 samples begin to relax below their T_g , even though it is not a complete relaxation. This is linked to topology freezing temperature (T_f), which is defined as the transition from solid to liquid as a result of bond

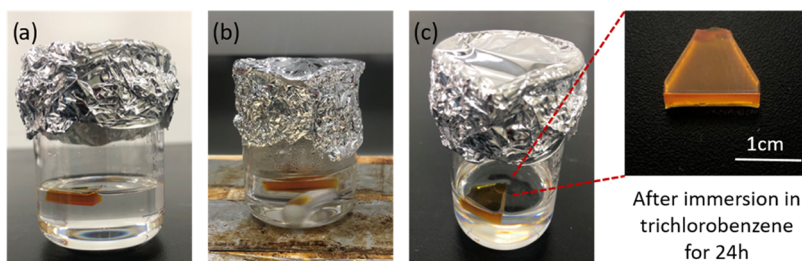


Figure 7. (a) VT-2 sample in trichlorobenzene after 24 h at RT (b) with continuous stirring at 80 °C and (c) VT-2 sample in trichlorobenzene after 4 h at 80 °C.

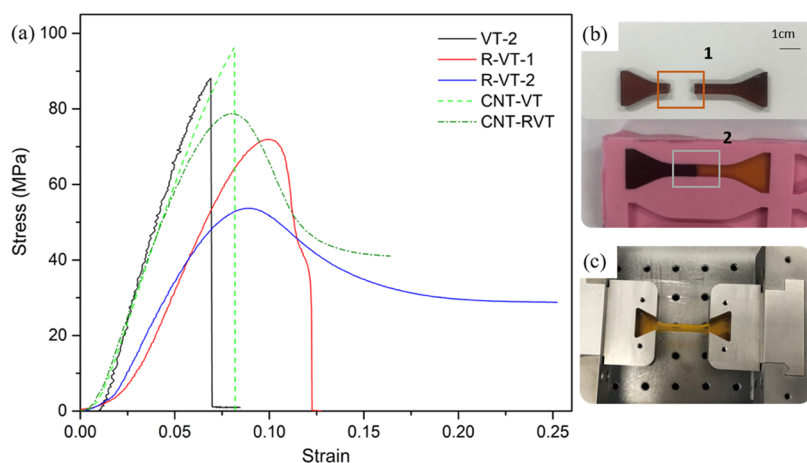


Figure 8. (a) Stress–strain curves of crosslinked, soft segment-introduced, and CNT-reinforced samples; (b) sample cut in half (1) and healing process (2); and (c) tensile testing of the samples.

exchange.^{2,24} For dynamic thermoset polymers, T_v is lower than T_g ,⁵¹ confirming the relaxation behavior in VT-2 and R-VT-1 samples, as the bond exchange may begin below T_g . Figure 6b depicts that G/G^0 values reach zero for both VT-2 and R-VT-1 samples, implying full stress relaxation above T_g . This is related to the increased bond exchange rate and segmental motion above T_g .² For the samples showing complete relaxation, the relaxation times are defined as the time required to relax 63% of initial stress² or to obtain $G/G^0 = 1/e$ with reference to the Maxwell model for viscoelastic fluids.^{19,52} The achieved relaxation times are found to be 4.05 min for VT-2 at 150 °C and 3.34 min for R-VT-1 at 80 °C. The R-VT-1 sample displays a higher relaxation rate than that of other samples, which can be attributed to the flexible chain backbone due to the soft segment portions. Consequently, the temperatures in healing and reshaping procedures are decided to be adequate for the network to relax completely and gain mobility.

3.1.6. Solvent Resistance. The chemical resistance of epoxy networks is examined to ensure that the rehealable epoxy network does not dissolve in the presence of a solvent yet and shows stress relaxation still. In a similar manner to the previous studies,^{23,53} a part of VT-2 and R-VT-1 are immersed in trichlorobenzene for 4 h first at RT and then at 80 °C with continuous stirring, Figure 7. No alteration is monitored in epoxy dynamic networks even after 24 h similar to conventional epoxy composites. This indicates the excellent solvent resistance and crosslinked network of dynamic epoxies with disulfide exchange bonds.

3.1.7. Micro-tensile Test. This research examines varying crosslink and CAN densities with the assistance of soft

segments and CNTs to achieve the required polymer mobility without sacrificing strength. Tensile tests are conducted using a Pyslotech micro-tensile testing machine and 10 kN load cell, until the complete failure of the samples. The testing speed is set as 100 mm/min, and the samples are prepared in a dumbbell shape of 4mm thickness and 60mm length, as shown in Figure 8c. Table 4 illustrates the average tensile strength for

Table 4. Tensile Strengths of Original and Rehealed Samples

sample	σ_{original} (MPa)	σ_{healed} (MPa)	healing efficiency (η -%)
VT-1	105.6 ± 8.1	2.4 ± 0.1	2.3
VT-2	91.9 ± 2.6	7.9 ± 1.6	8.6
VT-3	89.1 ± 3.6	8.6 ± 2.6	9.6
R-VT-1	69.9 ± 2.1	14.6 ± 2.4	20.9
R-VT-2	51.4 ± 1.2	19.3 ± 2.6	37.5
CNT-VT ^a	56.5 ± 7.2		
CNT-VT	95.7 ± 0.4	13.1 ± 1.4	13.7
CNT-RVT	75.4 ± 2.2	17.9 ± 0.7	23.7

^aCNT-VT produced without a surfactant.

at least three samples in each batch. VT-1 having the stoichiometric ratio exhibits the highest mechanical strength as expected due to its higher crosslink density, wherein increasing the CAN density leads to a decrease in tensile strength for VT-2 and VT-3 proportionally.

Optimizing the soft-to-hard segment ratio in the epoxy resin, R-VT-1 presents more ductility due to the flexible DGEPG chain segments, Figure 8. R-VT-1 demonstrates a 23% decrease in the ultimate tensile strength compared to that of

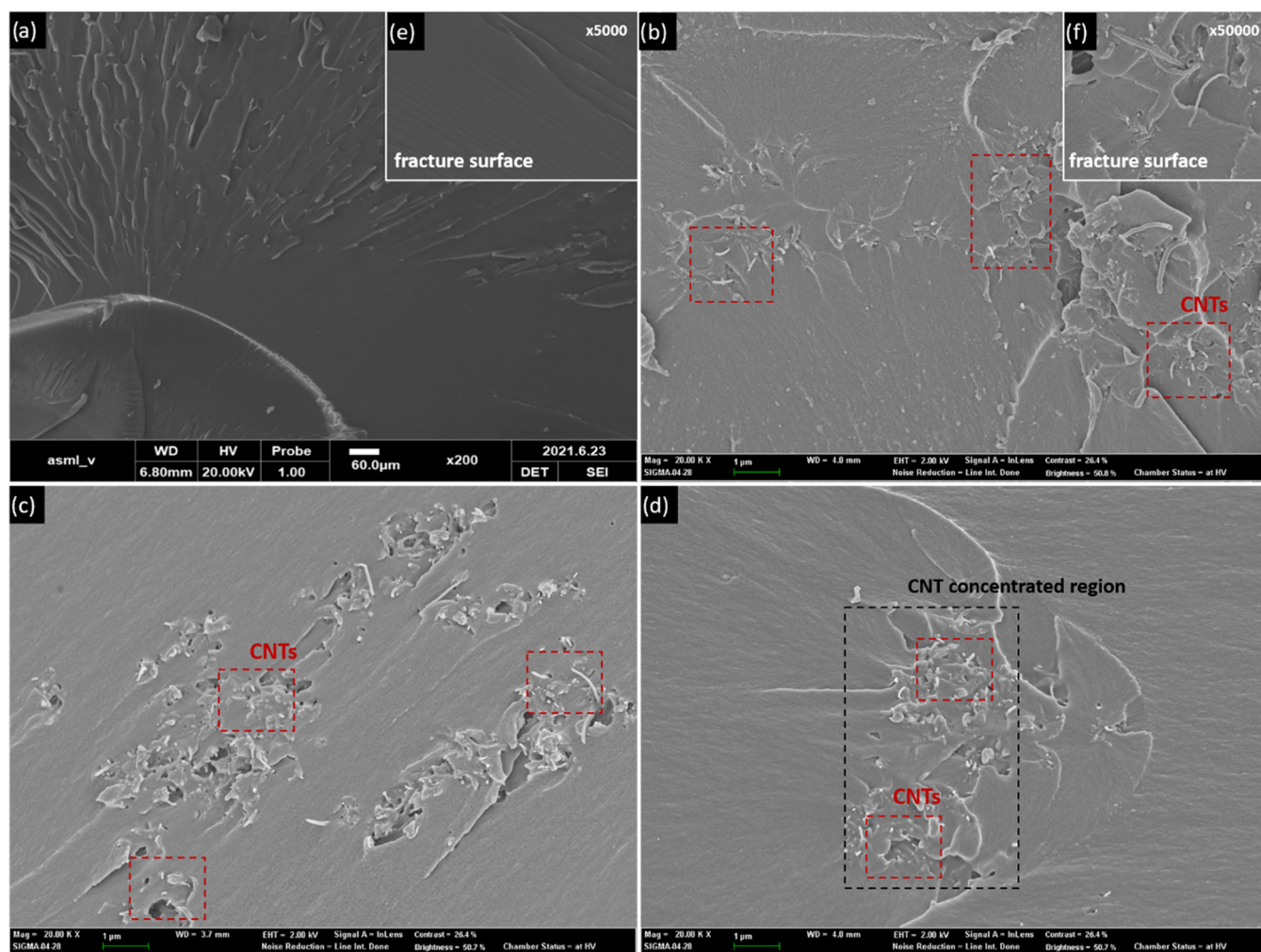


Figure 9. SEM images of the fracture surfaces of (a) neat VT-2, (b) CNT-VT with a surfactant, (c) CNT-RVT with a surfactant, and (d) CNT-VT without a surfactant.

VT-2. With increasing soft segment ratio, R-VT-2 displays more ductile behavior along with a lower ultimate tensile strength, **Figure 8**. Reinforcing the sample VT-2 with CNTs generates 4.1% enhancement in the ultimate tensile strength due to the nanotubes' individual high mechanical strength^{25,26} cooperating with the load carrying mechanism. The tensile strength of the CNT-RVT sample is increased nearly 8.0% even with a low weight ratio of CNTs. Similar effects are observed for CNT-reinforced epoxy in the literature.^{54,55} For this reason, introducing CNTs is considered an effective approach to compensate the strength and toughness for the soft segment-introduced R-VT samples. By this means, it is aimed to accomplish high healing and mechanical performances at the same time.

3.1.8. Morphological Characterization. The morphological characteristics of the epoxy networks are investigated by scanning electron microscopy (SEM). SEM images are taken at the cross-sectional areas with an accelerating voltage of 2 kV under high vacuum. The samples are prepared by first breaking them in half followed by coating a thin layer of gold. As shown in **Figure 9e**, the cross-sectional area of the neat VT shows a relatively more smooth fracture surface. Nonetheless, the failure of CNT-VT results in a rougher surface consisting of an epoxy layer and CNT/epoxy layer structure, **Figure 9f**. The difference between fracture surfaces of the neat VT and CNT-

VT is referred to the lower toughness of the neat sample. Moreover, the fracture surface of the CNT-VT sample gets distorted due to CNTs causing a more difficult crack propagation.⁵⁶ **Figure 9b** depicts that even though a surfactant is implemented and sonication is performed, CNTs stack more in some regions due to their high surface energy and hydrophobic surfaces.⁵⁷ Such stacking may cause a lower reinforcing effect than the estimated theoretical effect of CNTs in the polymer.³² Hence, it is crucial to understand the synergistic effect of CNTs in the network and their effect on the overall load carrying capability of nanocomposites.

When CNTs are dispersed directly in the resin without any functionalization, they tend to agglomerate and terminate with a nonhomogeneous structure (**Figure 9d**) due to their high aspect ratio along with van der Waals forces between nanotubes. This leads to a decrease in the mechanical performance, as given in **Table 4**, since CNT agglomerates behave as stress concentration points.⁴⁸ Contrarily, CNTs on the fracture surface of the samples synthesized with a surfactant, **Figure 9b**, appear to be more evenly distributed, promising a more efficient load transfer between the nanotube and the matrix.⁵⁸ Comparing **Figure 9b,c**, the CNT-VT sample is discovered to have a more homogeneous distribution state than that of CNT-RVT. Even though the dispersion of CNTs is less than ideal, CNT inclusion is still found to enhance the

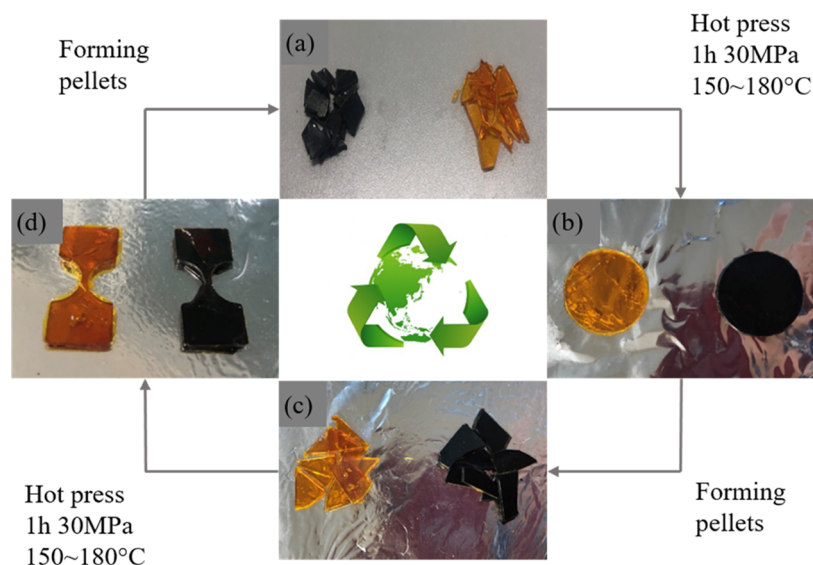


Figure 10. Repeatable reshaping process of neat and CNT-reinforced epoxy dynamic networks; (a) pellets produced from the original sample; (b) reshaped samples—1st cycle; (c) pellets produced from the reshaped sample; and (d) reshaped samples—2nd cycle.

toughness along with a potential increase in healing performance.

3.2. Rehealing. After applying the same healing procedure to Ref-Ep-1, Ref-Ep-2, and Ref-R-Ep samples, there was no healing observed at 150° and even 180 °C, justifying the role of disulfide metathesis in the healing mechanism, Figure S9, wherein VT-2 recovers its original strength of around 9% within disulfide bond exchanges. The healing observed in the VT-2 sample can be misapprehended as the curing of the unreacted species in a stoichiometric imbalance. However, it is proven clearly that the healing takes place due to disulfide bond exchange considering Ref-Ep-2. The Ref-Ep-2 sample having the same stoichiometric imbalance does not show any healing since there are no disulfide exchange bonds in the structure, Figure S9. This signifies that the unreacted species are not enough to exhibit healing by themselves.

At least three samples in each case are studied for healing, and the average values are presented in Table 4. VT-1 shows the lowest healing efficiency, which is associated with the relatively lower CAN density and higher crosslink density due to stoichiometry. A high crosslink density restrains the stress relaxation in the epoxy network and consequently the healing performance.³ Increased CAN density governs better healing of the broken samples, as VT-2 and VT-3 possess 8.6 and 9.6% healing efficiency, respectively. Moreover, CNT-VT presents 5.1% higher healing efficiency compared to that of the VT-2 sample, as expected from previous considerations.

Compared to crosslinked networks, soft segment-introduced samples present higher healing efficiency and relatively lower mechanical strength, as summarized in Table 4. Increased DGEPG contributes to flexibility and chain mobility since the crosslink density decreases proportionally. Owing to the increased DGEPG molar ratio, healing efficiency changes remarkably. Such an enhanced healing performance is in good correlation with the aforementioned relaxation behaviors of VT-2 and R-VT-1 samples. The R-VT-1 sample is capable of relaxation even under T_g , signifying that exchange reactions begin earlier than T_g , Figure 6a. The R-VT-1 sample shows a 20.9% recovery of the original strength after healing, wherein the efficiency is 37.5% for R-VT-2. It is attributed to the higher

flexibility of R-VT-2 since healing favors higher chain mobility and disulfide bond exchange. The increased healing efficiency was forecasted from the heat capacity increase results, Table 3, having higher motion of molecular chains. In a similar manner, CNT-RVT has a healing efficiency of 23.7% having more mobility than that of the R-VT-1 sample. Ultimately, CNT inclusion into R-VT compensates the loss in tensile strength and leads to enhanced healing. Considering other rehealable epoxy-related studies in the literature, this study provides a detailed explanation on the effects of both CNTs and soft segments on the healing mechanism simultaneously.

3.3. Reshaping. Once the healing behavior of dynamic networks is confirmed, reshaping is studied in a hot press. Similar to healing, reshaping is performed not only in dynamic networks but also in reference epoxy samples to point out the importance of the disulfide presence. As can be concluded from Figure S9, reference epoxy networks cannot be reshaped when there are no reversible disulfide exchange bonds in the structure.

As shown in Figure 10b, epoxy pellets are filled in a circular cross-section mold. Soft segment-introduced samples are heated to 150°C in a hot press and 30 MPa pressure is applied for 1 h. The same procedure is carried out for VT samples at 180 °C. All of the epoxy dynamic networks possess reshaping capability due to disulfide bond exchange. The reshaping process is repeated for a second time with the same samples. The resultant samples are in the dog-bone shape with a length of 25 mm and a thickness of 2mm. The width is 10 mm at the tips and 1 mm at the necking region, as shown in Figure 10d. A tensile test is performed using a Deben microtensile stage and 200 N load cell, and the testing speed is defined as 1.5 mm/min. Figure 11 demonstrates that tensile strengths are reduced for reshaped samples considering their original strengths. Still, the strengths are acceptable, considering that nearly 45% of the original strength is restored in the CNT-RVT sample after reshaping 2 times. A reduction in strength is unavoidable, yet the strengths were still comparable to those of the healed samples. The fabricated epoxy dynamic networks are determined to be capable of further utilization as a component for nonstructural applications.

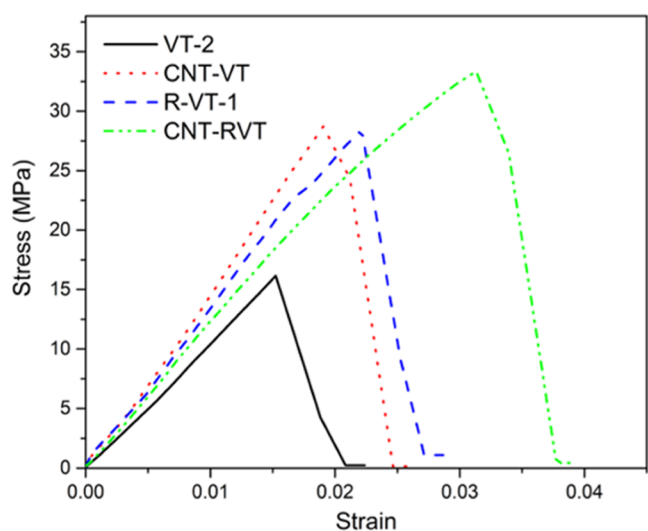


Figure 11. Tensile strength of 2 times reshaped samples.

To verify the properties of the reshaped samples, FTIR and DMA in the tension mode are conducted, Figures S2 and S8, respectively. FTIR spectra of the original and reshaped samples are quite similar, remarking that the epoxy network does not suffer from thermal decomposition after the reshaping process. T_g values of the reshaped samples are detected from the peak value of $\tan \delta$ curves and found to be 124.5 and 60.7 °C for VT-2 and R-VT-1 samples, respectively. T_g values of the reshaped samples are slightly higher than those of the original samples. The storage modulus is also observed to be higher than that of the original samples after one cycle of reshaping. This is attributed to the shortened macromolecules in its structure, which can rearrange easily and densely under applied heat and pressure conditions.^{59–61} It is verified that the reshaping process is repeatable, although repeated reshaping can generate degradation gradually after each time.⁶¹

4. CONCLUSIONS

In this study, healing and reshaping mechanisms of epoxy dynamic networks with reversible covalent adaptive networks are examined based on CAN density and crosslink density together with CNT inclusion. Various combinations of neat and CNT-reinforced epoxy dynamic networks are analyzed carefully to identify their thermomechanical and healing characteristics. It is crucial to point out that the tensile strengths of epoxy dynamic networks are at least 50 MPa even with a soft segment. Higher flexibility, lower crosslink density, and higher CAN density are found to be favorable for an enhanced healing behavior. VT samples with only a hard-segmented resin (DGEBA) exhibit a healing performance that is less than ideal. Introducing soft segments (DGEPG) into the existing network enhances the healing efficiency remarkably. Furthermore, it is proven that CNTs implement a lower T_g and higher mobility and thereby a higher healing efficiency. In addition to healing, epoxy dynamic networks display a repetitive reshaping capability, promoting the recyclability for environmental protection. This study offers a better understanding of tuning the stiffness of epoxy along with healing and reshaping, promising a reduced maintenance cost and prolonged lifetime for the industrial applications of epoxy.

■ ASSOCIATED CONTENT

Supporting Information

The Supporting Information is available free of charge at <https://pubs.acs.org/doi/10.1021/acsomega.2c03910>.

FTIR spectra of the reference and dynamic epoxy networks; original and reshaped samples; TGA curves of the reference and dynamic epoxy networks; DSC curves and heat capacity increase calculations; DMA traces of the original and reshaped epoxy dynamic networks; crosslink density estimation from DMA data; images of the reference epoxy networks after performing reshaping; and determination of healing temperature for dynamic epoxy networks (PDF)

■ AUTHOR INFORMATION

Corresponding Author

Gun Jin Yun – Department of Aerospace Engineering, Seoul National University, Seoul 08826, South Korea; Institute of Advanced Aerospace Engineering Technology, Seoul National University, Seoul 08826, South Korea; orcid.org/0000-0001-8387-3613; Phone: +82-2-880-8302; Email: gunjin.yun@snu.ac.kr

Authors

Cigdem Caglayan – Department of Aerospace Engineering, Seoul National University, Seoul 08826, South Korea

Geonwoo Kim – Department of Aerospace Engineering, Seoul National University, Seoul 08826, South Korea

Complete contact information is available at:

<https://pubs.acs.org/10.1021/acsomega.2c03910>

Notes

The authors declare no competing financial interest.

■ ACKNOWLEDGMENTS

This material is based upon work supported by the Air Force Office of Scientific Research under award number FA2386-20-1-4067. The authors thank the United States Air Force Office of Scientific Research for supporting this work financially. This work was also supported by the Institute of Engineering Research at Seoul National University and the BK21 Program funded by the Ministry of Education (MOE, Korea) and the National Research Foundation of Korea (NRF-419990513944). The authors are grateful for their support.

■ REFERENCES

- (1) Krishnakumar, B.; Sanka, R. V. S. P.; Binder, W. H.; Park, C.; Jung, J.; Parthasarthy, V.; Rana, S.; Yun, G. J. Catalyst free self-healable vitrimer/graphene oxide nanocomposites. *Composites, Part B* **2020**, *184*, No. 107647.
- (2) de Luzuriaga, A. R.; Martin, R.; Markaide, N.; Rekondo, A.; Cabañero, G.; Rodríguez, J.; Odriozola, I. Epoxy resin with exchangeable disulfide crosslinks to obtain reprocessable, repairable and recyclable fiber-reinforced thermoset composites. *Mater. Horiz.* **2016**, *3*, 241–247.
- (3) Liu, H.; Zhang, H.; Wang, H.; Huang, X.; Huang, G.; Wu, J. Weldable, malleable and programmable epoxy vitrimers with high mechanical properties and water insensitivity. *Chem. Eng. J.* **2019**, *368*, 61–70.
- (4) Safaei, F.; Khorasani, S. N.; Rahnama, H.; Neisiany, R. E.; Koochaki, M. S. Single microcapsules containing epoxy healing agent used for development in the fabrication of cost efficient self-healing epoxy coating. *Prog. Org. Coat.* **2018**, *114*, 40–46.

- (5) Ahangaran, F.; Hayaty, M.; Navarchian, A. H.; Pei, Y.; Picchioni, F. Development of self-healing epoxy composites via incorporation of microencapsulated epoxy and mercaptan in poly(methyl methacrylate) shell. *Polym. Test.* **2019**, *73*, 395–403.
- (6) Yang, Y.; Xu, Y.; Ji, Y.; Wei, Y. Functional epoxy vitrimers and composites. *Prog. Mater. Sci.* **2020**, No. 100710.
- (7) Chen, M.; Zhou, L.; Wu, Y.; Zhao, X.; Zhang, Y. Rapid Stress Relaxation and Moderate Temperature of Malleability Enabled by the Synergy of Disulfide Metathesis and Carboxylate Transesterification in Epoxy Vitrimers. *ACS Macro Lett.* **2019**, *8*, 255–260.
- (8) Pepels, M.; Filot, I.; Klumperman, B.; Goossens, H. Self-healing systems based on disulfide–thiol exchange reactions. *Polym. Chem.* **2013**, *4*, No. 4955.
- (9) Lu, L.; Pan, J.; Li, G. Recyclable high-performance epoxy based on transesterification reaction. *J. Mater. Chem. A* **2017**, *5*, 21505–21513.
- (10) Guadagno, L.; Vertuccio, L.; Naddeo, C.; Calabrese, E.; Barra, G.; Raimondo, M.; Sorrentino, A.; Binder, W. H.; Michael, P.; Rana, S. Self-healing epoxy nanocomposites via reversible hydrogen bonding. *Composites, Part B* **2019**, *157*, 1–13.
- (11) Ehrhardt, D.; Van Durme, K.; Jansen, J. F. G. A.; Van Mele, B.; Van den Brande, N. Self-healing UV-curable polymer network with reversible Diels-Alder bonds for applications in ambient conditions. *Polymer* **2020**, *203*, No. 122762.
- (12) Kuang, X.; Liu, G.; Dong, X.; Liu, X.; Xu, J.; Wang, D. Facile fabrication of fast recyclable and multiple self-healing epoxy materials through diels-alder adduct cross-linker. *J. Polym. Sci., Part A: Polym. Chem.* **2015**, *53*, 2094–2103.
- (13) Liu, Y.-L.; Chuo, T.-W. Self-healing polymers based on thermally reversible Diels–Alder chemistry. *Polym. Chem.* **2013**, *4*, No. 2194.
- (14) Bonab, V. S.; Karimkhani, V.; Manas-Zloczower, I. Ultra-Fast Microwave Assisted Self-Healing of Covalent Adaptive Polyurethane Networks with Carbon Nanotubes. *Macromol. Mater. Eng.* **2019**, *304*, No. 1800405.
- (15) Taynton, P.; Yu, K.; Shoemaker, R. K.; Jin, Y.; Qi, H. J.; Zhang, W. Heat- or water-driven malleability in a highly recyclable covalent network polymer. *Adv. Mater.* **2014**, *26*, 3938–3942.
- (16) Hu, J.; Mo, R.; Sheng, X.; Zhang, X. A self-healing polyurethane elastomer with excellent mechanical properties based on phase-locked dynamic imine bonds. *Polym. Chem.* **2020**, *11*, 2585–2594.
- (17) Azcune, I.; Odriozola, I. Aromatic disulfide crosslinks in polymer systems: Self-healing, reprocessability, recyclability and more. *Eur. Polym. J.* **2016**, *84*, 147–160.
- (18) de Luzuriaga, A. R.; Matxain, J. M.; Ruipérez, F.; Martin, R.; Asua, J. M.; Cabañero, G.; Odriozola, I. Transient mechanochromism in epoxy vitrimer composites containing aromatic disulfide crosslinks. *J. Mater. Chem. C* **2016**, *4*, 6220–6223.
- (19) Li, Z.-J.; Zhong, J.; Liu, M.-C.; Rong, J.-C.; Yang, K.; Zhou, J.-Y.; Shen, L.; Gao, F.; He, H.-F. Investigation on Self-healing Property of Epoxy Resins Based on Disulfide Dynamic Links. *Chin. J. Polym. Sci.* **2020**, *38*, 932–940.
- (20) Park, C.; Kim, G.; Jung, J.; Krishnakumar, B.; Rana, S.; Yun, G. J. Enhanced self-healing performance of graphene oxide/vitrimer nanocomposites: A molecular dynamics simulations study. *Polymer* **2020**, *206*, No. 122862.
- (21) Canadell, J.; Goossens, H.; Klumperman, B. Self-Healing Materials Based on Disulfide Links. *Macromolecules* **2011**, *44*, 2536–2541.
- (22) Lafont, U.; van Zeijl, H.; van der Zwaag, S. Influence of cross-linkers on the cohesive and adhesive self-healing ability of polysulfide-based thermosets. *ACS Appl. Mater. Interfaces* **2012**, *4*, 6280–6288.
- (23) Si, H.; Zhou, L.; Wu, Y.; Song, L.; Kang, M.; Zhao, X.; Chen, M. Rapidly reprocessable, degradable epoxy vitrimer and recyclable carbon fiber reinforced thermoset composites relied on high contents of exchangeable aromatic disulfide crosslinks. *Composites, Part B* **2020**, *199*, No. 108278.
- (24) Zhou, F.; Guo, Z.; Wang, W.; Lei, X.; Zhang, B.; Zhang, H.; Zhang, Q. Preparation of self-healing, recyclable epoxy resins and low electrical resistance composites based on double-disulfide bond exchange. *Compos. Sci. Technol.* **2018**, *167*, 79–85.
- (25) Yeh, M.-K.; Hsieh, T.-H.; Tai, N.-H. Fabrication and mechanical properties of multi-walled carbon nanotubes/epoxy nanocomposites. *J. Mater. Sci. Eng. A* **2008**, *483–484*, 289–292.
- (26) Cha, J.; Jun, G. H.; Park, J. K.; Kim, J. C.; Ryu, H. J.; Hong, S. H. Improvement of modulus, strength and fracture toughness of CNT/Epoxy nanocomposites through the functionalization of carbon nanotubes. *Composites, Part B* **2017**, *129*, 169–179.
- (27) Patnaika, S. S.; Swain, A.; Roy, T. Creep compliance and micromechanics of multi-walled carbon nanotubes based hybrid composites. *Compos. Mater. Eng.* **2020**, *2*, 141–162.
- (28) Grady, B. P. Effects of carbon nanotubes on polymer physics. *J. Polym. Sci., Part B: Polym. Phys.* **2012**, *50*, 591–623.
- (29) Wu, J.; Xiang, F.; Han, L.; Huang, T.; Wang, Y.; Peng, Y.; Wu, H. Effects of carbon nanotubes on glass transition and crystallization behaviors in immiscible polystyrene/polypropylene blends. *Polym. Eng. Sci.* **2011**, *51*, 585–591.
- (30) Khare, K. S.; Khare, R. Effect of carbon nanotube dispersion on glass transition in cross-linked epoxy-carbon nanotube nanocomposites: role of interfacial interactions. *J. Phys. Chem. B* **2013**, *117*, 7444–7454.
- (31) Montazeri, A.; Montazeri, N. Viscoelastic and mechanical properties of multi walled carbon nanotube/epoxy composites with different nanotube content. *Mater. Des.* **2011**, *32*, 2301–2307.
- (32) Miyagawa, H.; Drzal, L. T. Thermo-physical and impact properties of epoxy nanocomposites reinforced by single-wall carbon nanotubes. *Polymer* **2004**, *45*, 5163–5170.
- (33) Cha, J.; Kim, J.; Ryu, S.; Hong, S. H. Comparison to mechanical properties of epoxy nanocomposites reinforced by functionalized carbon nanotubes and graphene nanoplatelets. *Composites, Part B* **2019**, *162*, 283–288.
- (34) Bai, Y.; Lin, D.; Wu, F.; Wang, Z.; Xing, B. Adsorption of Triton X-series surfactants and its role in stabilizing multi-walled carbon nanotube suspensions. *Chemosphere* **2010**, *79*, 362–367.
- (35) Geng, Y.; Liu, M. Y.; Li, J.; Shi, X. M.; Kim, J. K. Effects of surfactant treatment on mechanical and electrical properties of CNT/epoxy nanocomposites. *Composites, Part A* **2008**, *39*, 1876–1883.
- (36) Ma, Z.; Wang, Y.; Zhu, J.; Yu, J.; Hu, Z. Bio-based epoxy vitrimers: Reprocessability, controllable shape memory, and degradability. *J. Polym. Sci., Part A: Polym. Chem.* **2017**, *55*, 1790–1799.
- (37) Zhang, Y.; Yuan, L.; Liang, G.; Gu, A. Developing Reversible Self-Healing and Malleable Epoxy Resins with High Performance and Fast Recycling through Building Cross-Linked Network with New Disulfide-Containing Hardener. *Ind. Eng. Chem. Res.* **2018**, *57*, 12397–12406.
- (38) Doblies, A.; Boll, B.; Fiedler, B. Prediction of Thermal Exposure and Mechanical Behavior of Epoxy Resin Using Artificial Neural Networks and Fourier Transform Infrared Spectroscopy. *Polymer* **2019**, *11*, No. 363.
- (39) Abdollahi, H.; Salimi, A.; Barikani, M.; Samadi, A.; Hosseini Rad, S.; Zanjanijam, A. R. Systematic investigation of mechanical properties and fracture toughness of epoxy networks: Role of the polyetheramine structural parameters. *J. Appl. Polym. Sci.* **2018**, *136*, No. 47121.
- (40) Gonzalez, M. G.; Cabanelas, J. C.; Baselga, J. Applications of FTIR on epoxy resins identification monitoring the curing process phase separation and water uptake. In *Infrared Spectroscopy - Materials Science, Engineering and Technology*; Theophile, T., Ed.; InTech, 2012.
- (41) Boonlert-Uthai, T.; Samthong, C.; Somwangthanaroj, A. Synthesis, Thermal Properties and Curing Kinetics of Hyperbranched BPA/PEG Epoxy Resin. *Polymers* **2019**, *11*, No. 1545.
- (42) Ciecierska, E.; Boczkowska, A.; Kurzydowski, K. J.; Rosca, I. D.; Van Hoa, S. The effect of carbon nanotubes on epoxy matrix nanocomposites. *J. Therm. Anal. Calorim.* **2013**, *111*, 1019–1024.
- (43) Yang, S.-Y.; Ma, C.-C. M.; Teng, C.-C.; Huang, Y.-W.; Liao, S.-H.; Huang, Y.-L.; Tien, H.-W.; Lee, T.-M.; Chiou, K.-C. Effect of functionalized carbon nanotubes on the thermal conductivity of epoxy composites. *Carbon* **2010**, *48*, 592–603.

- (44) Wang, Z. K.; Lv, Q.; Chen, S. H.; Li, C. L.; Sun, S. Q.; Hu, S. Q. Effect of Interfacial Bonding on Interphase Properties in SiO₂/Epoxy Nanocomposite: A Molecular Dynamics Simulation Study. *ACS Appl. Mater. Interfaces* **2016**, *8*, 7499–7508.
- (45) Gao, B.; Yang, J.; Chen, Y.; Zhang, S. Oxidized cellulose nanocrystal as sustainable crosslinker to fabricate carboxylated nitrile rubber composites with antibiosis, wearing and irradiation aging resistance. *Composites, Part B* **2021**, *225*, No. 109253.
- (46) Zhang, C.; Tang, Z.; Guo, B. High-performance rubber/boehmite nanoplatelets composites by judicious in situ interfacial design. *Compos. Sci. Technol.* **2017**, *146*, 191–197.
- (47) Fragiadakis, D.; Bokobza, L.; Pissis, P. Dynamics near the filler surface in natural rubber-silica nanocomposites. *Polymer* **2011**, *52*, 3175–3182.
- (48) Song, Y. S.; Youn, J. R. Influence of dispersion states of carbon nanotubes on physical properties of epoxy nanocomposites. *Carbon* **2005**, *43*, 1378–1385.
- (49) Zhang, Y.-C.; Zheng, D.; Pang, H.; Tang, J.-H.; Li, Z.-M. The effect of molecular chain polarity on electric field-induced aligned conductive carbon nanotube network formation in polymer melt. *Compos. Sci. Technol.* **2012**, *72*, 1875–1881.
- (50) Mathew, V. S.; George, S. C.; Parameswaranpillai, J.; Thomas, S. Epoxidized natural rubber/epoxy blends: Phase morphology and thermomechanical properties. *J. Appl. Polym. Sci.* **2014**, *131*, No. 39906.
- (51) Denissen, W.; Winne, J. M.; Du Prez, F. E. Vitrimers: permanent organic networks with glass-like fluidity. *Chem. Sci.* **2016**, *7*, 30–38.
- (52) Zhao, S.; Abu-Omar, M. M. Recyclable and Malleable Epoxy Thermoset Bearing Aromatic Imine Bonds. *Macromolecules* **2018**, *51*, 9816–9824.
- (53) Montarnal, D.; Capelot, M.; Tournilhac, F.; Leibler, L. Silica-like malleable materials from permanent organic networks. *Science* **2011**, *334*, 965–968.
- (54) Singh, N. P.; Gupta, V. K.; Singh, A. P. Graphene and carbon nanotube reinforced epoxy nanocomposites: A review. *Polymer* **2019**, *180*, No. 121724.
- (55) Guo, P.; Song, H.; Chen, X. Interfacial properties and microstructure of multiwalled carbon nanotubes/epoxy composites. *J. Mater. Sci. Eng. A* **2009**, *517*, 17–23.
- (56) Zhou, Y.; Pervin, F.; Lewis, L.; Jeelani, S. Experimental study on the thermal and mechanical properties of multi-walled carbon nanotube-reinforced epoxy. *J. Mater. Sci. Eng. A* **2007**, *452-453*, 657–664.
- (57) Cheon, J. Y.; Ku, N.; Jung, Y.; Lee, K.; Kim, T. Hydrophilic treatment for strong carbon nanotube fibers. *Funct. Compos. Struct.* **2021**, *3*, No. 025002.
- (58) Gong, X.; Liu, J.; Baskaran, S.; Voise, R. D.; Young, J. S. Surfactant-Assisted Processing of Carbon Nanotube/ Polymer Composites. *Chem. Mater.* **2000**, *12*, 1049–1052.
- (59) Li, H.; Zhang, B.; Yu, K.; Yuan, C.; Zhou, C.; Dunn, M. L.; Qi, H. J.; Shi, Q.; Wei, Q. H.; Liu, J.; Ge, Q. Influence of treating parameters on thermomechanical properties of recycled epoxy-acid vitrimers. *Soft Matter* **2020**, *16*, 1668–1677.
- (60) Di Mauro, C.; Malburet, S.; Graillet, A.; Mija, A. Recyclable, Repairable, and Reshapable (3R) Thermoset Materials with Shape Memory Properties from Bio-Based Epoxidized Vegetable Oils. *ACS Appl. Bio Mater.* **2020**, *3*, 8094–8104.
- (61) Zhang, B.; Yuan, C.; Zhang, W.; Dunn, M. L.; Qi, H. J.; Liu, Z.; Yu, K.; Ge, Q. Recycling of vitrimer blends with tunable thermomechanical properties. *RSC Adv.* **2019**, *9*, 5431–5437.